Lifetime measurements in 110Cd

S. Harissopulos, A. Dewald, A. Gelberg, P. von Brentano, K. O. Zell, C. Kalfas

Lifetime measurements in ^{110}Cd

S. Harissopulos [a], A. Dewald [b], A. Gelberg [b],
P. von Brentano [b], K. O. Zell [b] and C. Kalfas [a]

[a] *Institute of Nuclear Physics, N.C.S.R. "Demokritos",*
POB 60228, GR-15310 Aghia Paraskevi, Athens, Greece
[b] *Institut für Kernphysik, Universität zu Köln, D-50937 Cologne, Germany*

Abstract

Mean lifetimes for the lowest 6 yrast band members in ^{110}Cd have been measured using the Recoil Distance Doppler Shift technique (RDDS). The data have been analyzed via the Differential Decay Curve Method (DDCM). The transition probabilities deduced from the data for the ground band E2 γ-rays are in rather good agreement with the predictions of the U(5)-limit of interacting boson model-1 (IBM-1).

1 Introduction

Lifetime measurements of excited nuclear states are very important for our understanding of nuclear structure: The main goal of these measurements is to test the predictions of different nuclear models in terms of transition probabilities. As schematically shown in fig. 1, by carrying out a lifetime measurement the mean lifetime τ of an excited level i is determined. Further, using the simple eq. 1 of fig. 1 one can deduce the "experimental" value for the reduced transition probability $B(L)_{EXPM}$ of the γ-ray with multipolarity L and energy E_γ through which state i is deexcited to state f. On the other hand, "theory", i.e. a certain nuclear model, uses its wavefunctions Ψ_i and Ψ_f to "describe" the initial level i and the final level f. Then, by means of the well know electromagnetic operator $M(L)$ a theoretical, i.e. a calculated value $B(L)_{THEOR}$ can be provided for the respective reduced transition probability by the model in consideration. Hence, by comparing experimental $B(L)$ values with calculated ones different nuclear models can be tested.

Nucleus ^{110}Cd has been characterized by Arima and Iachello in [1], as one of the best examples of nuclei resambling the U(5) symmetry of the so-called
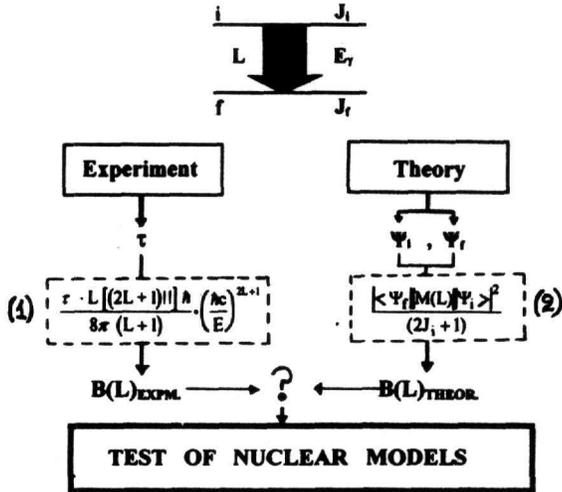
Fig. 1. *The goal of lifetime measurements*

"Interacting Boson Model-1" (IBM-1). This assignment was based mainly on the excitation energies and branching ratios of the low-lying collective states of ^{110}Cd. According to the above mentioned features of ^{110}Cd our aim by choosing this nucleus is twofold; firstly, to follow the evolution of the $B(E2)$ values along its yrast line and secondly to test further the predictions of the U(5) limit of IBM-1 in terms of transition probabilities. IBM-1 is well known for its so-called "limits", which correspond to certain "geometrical" descriptions of nuclear excitation. These limits are shown schematically in fig. 2. According to IBM-1 a nucleus resamling the U(5) symmetry "looks" like a vibrating nucleus (see fig. 2).

In order to experimentally determine a mean lifetime τ, different methods depending on the order of magnitude of τ have to be chosen. In our case, the mean lifetimes τ expected were in the 1 ps-1 ns range. Hence, the most appropriate method for measuring the lifetimes of interest was the so-called Recoil-Distance Doppler Shift method (RDDS). Details on this method, often called also plunger method, can be found in [2,3]

2 Experiments

The experiment was carried out at the FN Van de Graaff Tandem accelerator at the University of Cologne. The experimental setup is shown in fig. 3. The

By using group theory methods one can obtain analytical solutions in three "extreme" cases known as "limits" of IBM-1. These are:

I. U(5)-limit
II. SU(3)-limit
III. O(6)-limit

Each limit corresponds to a "geometrical" description of nuclear excitation:

U(5) - limit : vibrating nucleus
SU(3)- limit : rotating nucleus having either a prolate or an oblate shape
O(6)- limit : "something" between a prolate and an oblate nuclear shape
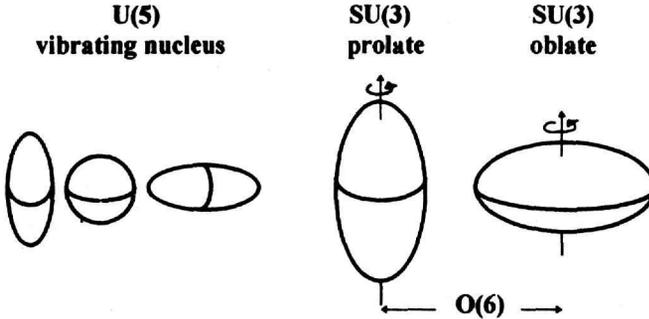

Fig. 2.   *Limits in IBM-1*

plunger device used in the present RDDS-measurement is described in [4]. At the beam energy used (E(^{13}C)=50 MeV) excited states in ^{110}Cd as well as in ^{109}Cd nucleus have been populated via the ^{100}Mo(^{13}C,3n) and ^{100}Mo(^{13}C,4n) reactions respectively.

As shown in fig. 3 three Ge detectors, each having a relative efficiency of about 18% and an energy resolution of about 2 keV for a 1408 keV γ-ray were used to measure γ-singles spectra at 24 different target-to-stopper distances (plunger distances) in the range 2.9 μm-8 mm. Fig. 3 shows also three different γ-singles spectra taken with the detector placed at 0° at plunger distances of a) $d = 6.1$ μm, b) $d = 73.9$ μm and c) $d = 8$ mm. In these spectra the Doppler-shifted and unshifted components of γ-transitions in the yrast line of ^{110}Cd are labeled with letters "s" and "u" respectively. Numbers in parenthesis indicate the enrgy in keV of some γ-rays depopulating states in ^{109}Cd. Numbers 633 and 876 are the energies in keV of the $2_1^+ \rightarrow 0_1^+$ and $4_1^+ \rightarrow 2_1^+$ γ-transitions of ^{108}Cd nucleus which is also produced due to a small admixture in ^{98}Mo of the target. Peaks indicated as [x] are mainly γ-rays due to activation.

The relative intensities of the γ-transitions of interest have been measured in a second independent experiment, in a so-called "intensity measurement". Hereby, γ-singles spectra were taken by means of one Ge detector placed at 55° with respect to the beam axis. The target used was a 0.6 mg/cm^2 thick

113

Target : 99% enriched in ^{100}Mo self supporting foil
Thickness ≈ 0.6 mgr/cm^2

Stopper : 2 mg/cm^2 tantalum foil

Beam stopper : 40 mg/cm^2 tantalum foil.
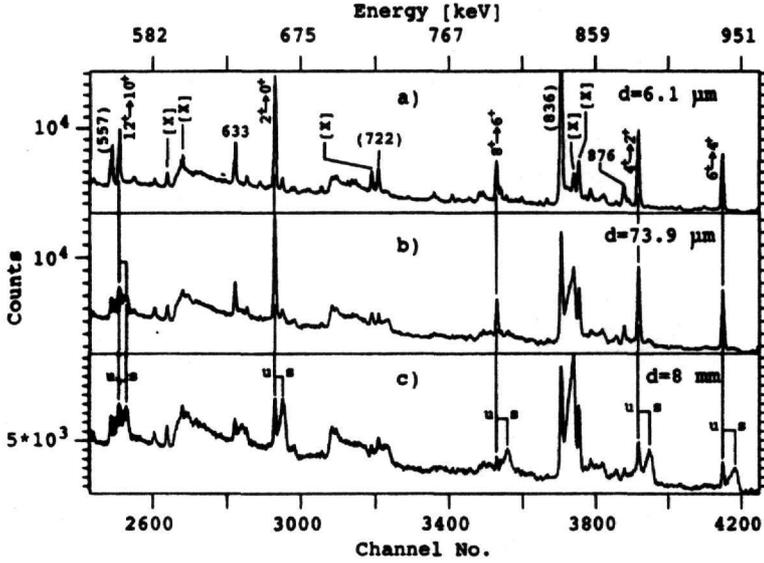
Reactions : ^{100}Mo $(^{13}C, \frac{3n}{4n})$ $^{110}_{109}Cd$, $E(^{13}C) = 50$ MeV

SETUP

Fig. 3.   Experimental setup and typical γ-singles spectra of the present RDDS measurement

^{100}Mo foil (98% enriched) rolled onto a 4.3 mg/cm^2 thick gold foil. The latter gold foil was backed by a 93 mg/cm^2 thick Bi-foil. The distance between target and detector was, as in the case of the former RDDS measurement, about 15 cm.

3 Data analysis

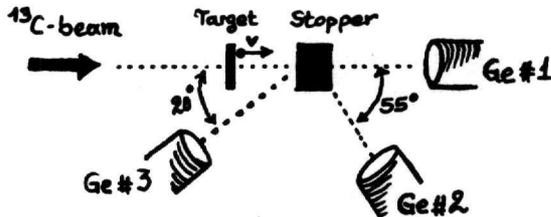In compound nucleus reactions the produced higly excited nuclei deexcite mainly via γ-cascades. Hence, when determining the mean lifetime of a certain excited state corrections due to the cascade feeding from higher lying levels have to be taken into account. This corrections lead to rather comlpicated expressions describing the decay of the level of consideration (see e.g. in [2,3]). Due to the above mentioned feeding corrections, the decay curve of the state of interest has to be described by a function which depends not only on the lifetime of this state but also on the lifetimes of all other feeding levels. Clearly, the data analysis consists of fitting all observed decay curves with a set of coupled differential equations, i.e. the individual lifetimes are determined by a χ^2 analysis. Such a procedure however possesses limits on the number of free parameters, when dealing with a complex feeding pattern. Furthermore one gets no hint on systematic errors since in many cases it is possible to obtain a rather good fit with completely false feeding assumptions.

In order to avoid such problems the data of the present work have been analysed according to the so-called *Differential Decay-Curve Method* (DDCM), which has been proposed recently [5] for determining mean lifetimes from plunger measurements. DDCM has been proved to be a rather transparent and a reliable method of analysis of Doppler-shift timing experiments. The main advantage of DDCM is its ability to "detect" systematic errors, which in the conventional analysis could not have been "found". As DDCM is discussed in details elsewhere [5,6], only the last "step" of this method is here outlined. According to this step of DDCM, a mean lifetime τ can be determined for an excited level i at every plunger distance x, where γ-spectra were taken, by using the equations given in fig. 4:

In order to understand the quantities used in these eqs. a schematic decay scheme, shown also in fig. 4, is necessary. Hereby, a level L_i is fed from levels L_h by γ-transitions noted as $(L_h \rightarrow L_i)$. Level L_i is further deexcited to levels L_j via γ-transitions $(L_i \rightarrow L_j)$. $Q_{ij}(x)$ and $Q_{hi}(x)$ are the experimental decay curves of the depopulating transitions $(L_i \rightarrow L_j)$ and the populating transitions $(L_h \rightarrow L_i)$ respectively. $U_{ij}(x)$ and $S_{ij}(x)$ are the intensities of the Doppler-unshifted and Doppler-shifted components respectively of the γ-transition $(L_i \rightarrow L_j)$. These components are often called "stop"and "flight" peak respectively. Quantity b_{ij} is the branching ratio of the transition $(L_i \rightarrow L_j)$ in consideration and v is the mean velocity of the recoiling nuclei. In addition, J_{hi} and J_{ij} are the intensities measured at 55°, i.e in an intensity measurement, for the respective γ-rays $(L_h \rightarrow L_i)$ and $(L_i \rightarrow L_j)$. Quantity $dQ_{ij}(x)/dx$ is the first derivative of the experimental decay curve $Q_{ij}(x)$.

In the present work the experimental decay curves $Q_{ij}(x)$ have been deter-

THE DIFFERENTIAL DECAY CURVE METHOD (D.D.C.M)
for the analysis of recoil distance doppler-shift data
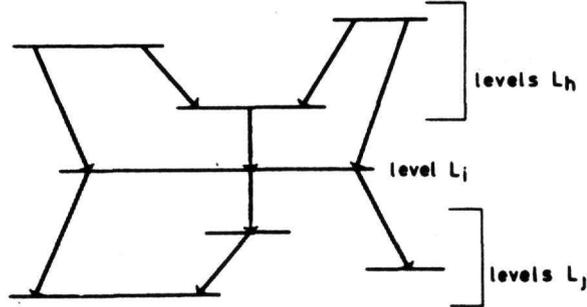
The last "step" in D.D.C.M.

$$\tau(x) = -\frac{Q_{ij}(x) - b_{ij}\left(\sum_h \left(\frac{J_{hi}}{J_{ij}}\right) Q_{hi}(x)\right)}{v \cdot \left(\frac{dQ_{ij}(x)}{dx}\right)} \quad , \qquad (1)$$

$$Q_{ab}(x) := \text{Experimental decay curve} = \frac{U_{ab}(x)}{U_{ab}(x) + S_{ab}(x)} \qquad (2)$$

Fig. 4. *DDCM analysis of RDDS data*

mined according to the procedure proposed by Dewald *et al.* in [7] using "difference" γ-singles spectra, which have been firstly normalized by means of the intensity of the 260 keV γ-ray of ^{109}Cd nucleus. This transition depopulates a very long lived $11^-/2$ isomeric state with $T_{1/2} = 8$ μs [8]. The intensities J_{hi} and J_{ij} as well as the branching ratios b_{ij} involved in the analysis have been determined, as already mentioned above, in an extra intensity measurement. The mean recoil velocity v has been derived from the Doppler-shift of some strong γ-transitions present in the γ-singles spectra: A v/c = 0.70(5)% was found.

As reported in [5] the first derivative $dQ_{ij}(x)/dx$ of an experimental decay curve $Q_{ij}(x)$ can be derived from the decay curve $Q_{ij}(x)$ by calculating the first derivative $dG(x)/dx$ of a continuously differentiable function $G(x)$: This function is obtained by fitting several second order polynomials over seperate intervals to the measured $Q_{ij}(x)$ data points. In the present work, the first derivatives $dG(x)/dx$ been obtained via such a fitting procedure carried out by means of code APATHIE [9]

From eq. 1, of fig. 4 it can be clearly seen that when applying DDCM one

116

actually determines at each plunger distance x, a value for the mean lifetime τ. These $\tau(x)$ data points have of course to lie, within statistical errors, on a straight line when considering a certain exited level: When this is not the case, then either the decay curves have not been corrected for various effects arising usually in plunger measurements, or other systematic errors are present in the data analysis. This is actually the main advantage in applying DDCM: This method enables to "detect" possible systematic errors the majority of which can not be "seen" in a "conventional" data analysis. As already shown in [10], systematic errors may arise in the data analysis when the contribution of the so-called side feeding intensity J_i^{sf}, i.e. the feeding from contiuum and/or by unobserved weak discrete transitions, to the decay curves has not been assessed correctly. J_i^{sf} is defined by the following equation:

$$J_i^{sf} = \sum_j J_{ij} - \sum_h J_{hi} \tag{1}$$

According to [10], side feeding is not *à priori* negligible, especially when the relative side feeding intensity of the level in consideration L_i is not small enough, i.e. when $J_i^{sf}/\sum_j J_{ij} \geq 5\%$. In such cases and according to the findings of [10] the side feeding of level L_i can be simulated by an "effective" side feeding decay curve, noted here as $Q_i^{sf}(x)$, which is to be obtained as the weighted average of the decay curves $Q_{hi}(x)$ of the discrete transitions ($L_h \rightarrow L_i$) which feed into the level L_i. $Q_i^{sf}(x)$ is to be calculated according to the following eq. 2.

$$Q_i^{sf}(x) = J_i^{sf} \left[b_{ij} \sum_h (\frac{J_{hi}}{J_{ij}}) Q_{hi}(x) \right] \tag{2}$$

In our analysis special care was focussed on the problem of side feeding: The relative side feeding intensities, of all levels studied in the present work are given in table 1. As it can be seen there, the relative side feeding intensities of the ground band members up to 8^+ state were small enough so that the contribution of side feeding to the decay curves of these states could be neglected. This, however, was not the case for the 10_1^+ and 12_1^+ states. For these states an effective side feeding decay curve was calculated according to eq. 2 and taking into account that these levels are fed by only one discrete feeding transition.

The application of DDCM in our data is demonstated in fig. 5 for the case of the 10_1^+ state. In part a) of this figure one can see the experimental decay curves $Q_{10}(x)$ (data points) of the 10_1^+ and 12_1^+ levels. The solid curves are the respective continuously differentiable functions $G_{10}(x)$ and $G_{12}(x)$ fitted to the data points via code APATHIE, as already mentioned above. The first derivative $dQ_{ij}(x)/dx$ of the 10_1^+ state, i.e. the values $dG_{10}(x)/dx$, after being multiplied by the recoil velocity v, is shown in part c) of fig. 5. These data points actually represent the denominator values of eq. 1 of fig. 4, whereas
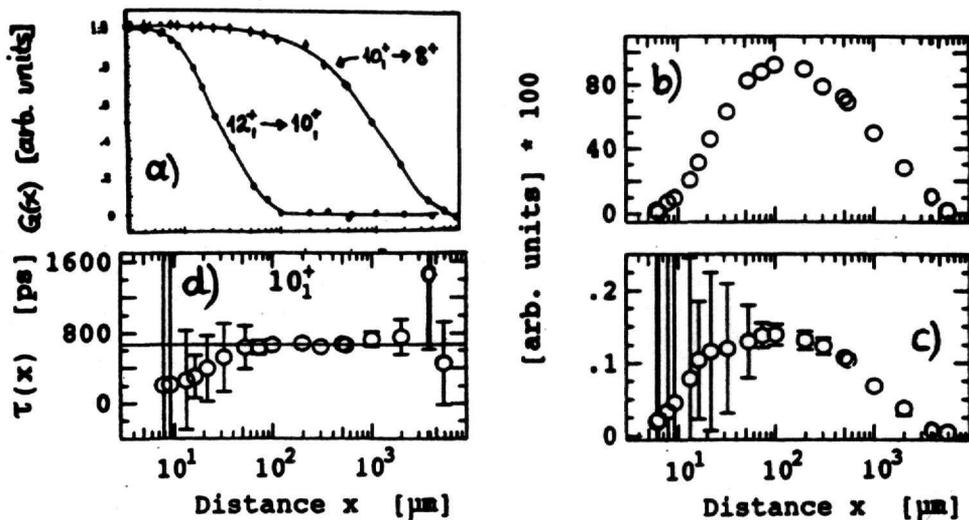
117

Fig. 5. *DDCM analysis of the 10_1^+ state in ^{110}Cd.*

the numerator of the same eq. is shown in part b) of fig. 5. The result of the deviation of the data points shown in part b) over the respective data points shown in part c), i.e. the $\tau(x)$ "curve" of the 10_1^+ state is shown in part d).

4   Results and Discussion

The experimental $\tau(x)$-curves determined in the present work for the yrast band members up to 12_1^+ state are shown in fig. 6. As shown in this fig. the $\tau(x)$-values of all levels investigated, do not indicate any systematic errors: The data points $\tau(x)$ lie indeed, within statistical errors, on a straight line. Due to statistics, these errors are, especially in the case of 4_1^+ and 6_1^+ states, relatively large. The mean lifetimes τ deduced as the weighted average of the $\tau(x)$ values are summarized in table 1. For the data analysis, the level scheme reported in [11] has been adopted. In fig. 7, it is shown part of the level scheme of ^{110}Cd in which all the γ-transitions involved in our analysis are included.

The mean lifetime of the 2_1^+ state ($\tau = 8.7(12)$ *ps*) determined here, is statistically in agreement with these reported in [11] ($\tau = 9.2(6)$ *ps*) and in [12] ($\tau = 7.78(10)$ *ps*). The latter value has been deduced from the $B(E2)$ values determined in a Coulomb excitation experiment, whereas the mean lifetime reported in [11] has been measured in a plunger measurement. The mean lifetime
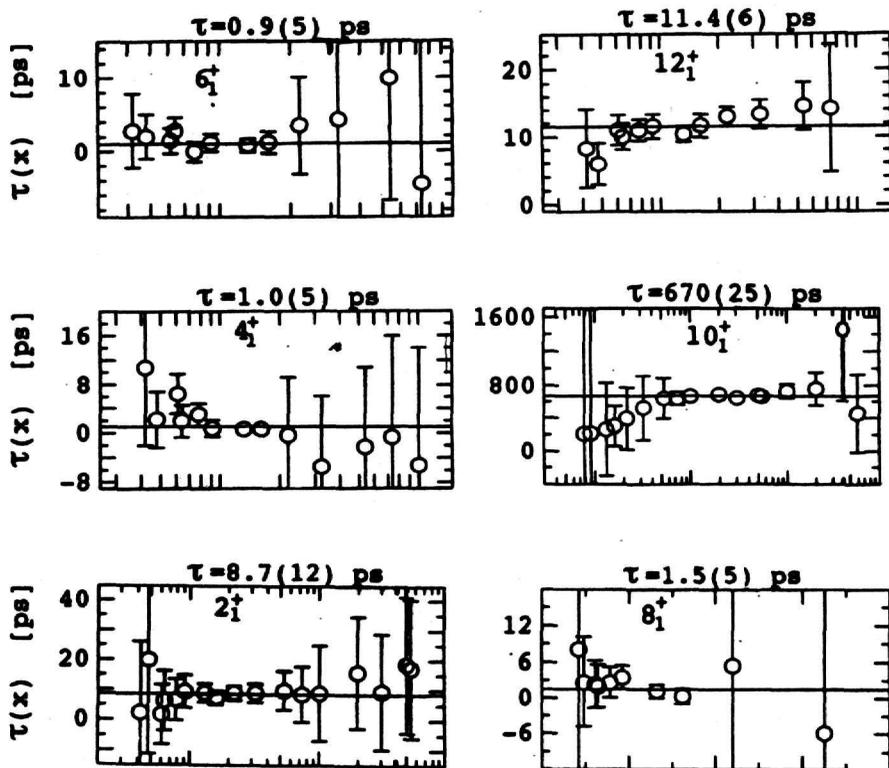
Fig. 6. $\tau(x)$-curves determined for in ^{110}Cd.

of 4_1^+ state ($\tau = 1.0(5)$ ps) determined in the present work is also in agreement with this reported in [12] ($\tau = 1.05(13)$ ps). For the 6_1^+ and 8^+ states at $E_x = 2480$ keV and $E_x = 3275$ keV excitation energies respectively (see fig. 7), mean lifetimes of $0.9(5)$ ps and $1.5(5)$ ps have been here determined, for the first time.

The mean lifetime determined in the present work for the 10_1^+ state ($\tau = 670(25)$ ps) do not justify the findings of [11], where a longer mean lifetime ($\tau = 800(40)$ ps) has been reported for the state considered. Our result for the mean lifetime of the 12_1^+ state ($\tau = 11.4(6)$ ps) is statistically in agreement with the respective mean lifetime reported in [11] ($\tau = 12.0(6)$ ps). For the 14_1^+ state at $E_x = 5026$ keV and the 10_2^+ level at $E_x = 4078$ keV only an upper limit of $\tau \leq 3$ ps and $\tau \leq 4$ ps respectively could be determined in the present work, since the decay curves of their precursor states could not be measured. This was also the case for the 7^- and 5^- states at $E_x = 2879$ keV

119

Fig. 7. *Partial level scheme of* ^{110} *Cd (from. [11]). The width of the arrows represends the relative intensity of the corresponding transition. The excitation energy of each of the three different* 8^+ *states is given in parenethesis.*

and $E_x = 2540$ keV, for which upper limits of 1018(101) *ps* and 885(120) *ps* respectively could be derived. These upper limits have been extracted for all above states by fitting a single exponential function to the respective decay curves.

The $B(E2)$ values determined in the present work for the lowest $E2$ yrast band γ-transitions are given in table 1. According to these values, an increase in collectivity occurs up to the 8^+ state at $E_x = 3275$ keV (see fig. 7). Above this level one distinguishes between a "slow" and a "fast" pathway. The former proceeds through the 335 keV γ-ray deexciting the 10_1^+ state ($\tau_{10^+} = 670(25)$ ps, $B(E2; 335 \text{ keV}) = 6.6^{+0.4}_{-0.3}$ W.u.), whereas the latter via the 802 keV γ-line. For the 802 *keV* γ-transition, through which the 10_2^+ level is deexcited, only a lower limit of $B(E2; 802 \text{ keV}) > 16$ W.u. could be here determined. This limit is in agreement with the high transition rate of $B(E2; 802 \text{ keV}) = 74(24)$ W.u. reported in [11]. Above the 10_1^+ state the collectivity "recovers": A high transition probability of $B(E2) = 41(2)$ W.u. has been here determined for the $12_1^+ \rightarrow 10_1^+$ γ-transition (E$_\gamma$ = 561 keV).

In fig. 8 the relative $B(E2)$ values measured here for ^{110}Cd, i.e. the experi-
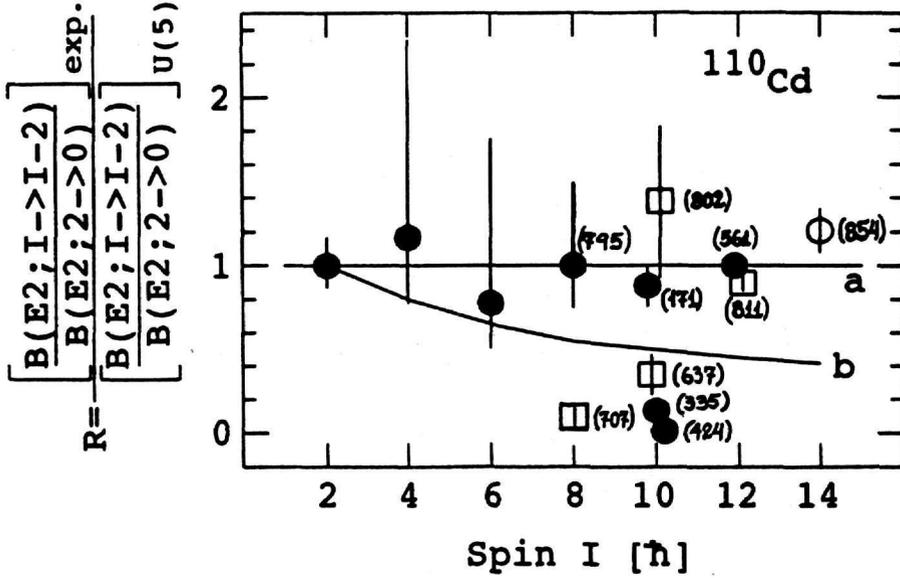
120

Fig. 8. *Plot of the ratios $R(I)$ as defined in eq. 4 vs. spin I. Filled circles have been obtained in the present work, whereas open squares and the open circle at $I = 14$ $\hbar$ have been adopted from [11]*

mental ratios

$$R_{exp.}(I) = \frac{B(E2; I \rightarrow I - 2)_{exp.}}{B(E2; 2_1^+ \rightarrow 0_1^+)_{exp.}} \tag{3}$$

are compared with the respective ratios predicted by the U(5)-limit of IBM-1. Hence, in fig 8., the ratios

$$R(I) = \frac{R_{exp.}(I)}{R_{U(5)}(I)} = \frac{\left[\frac{B(E2; I \rightarrow I - 2)}{B(E2; 2_1^+ \rightarrow 0_1^+)} \right]_{exp.}}{\left[\frac{B(E2; I \rightarrow I - 2)}{B(E2; 2_1^+ \rightarrow 0_1^+)} \right]_{U(5)}} \tag{4}$$

are plotted vs. (initial) spin I. Hereby, the filled circles correspond to data measured in the present work, whereas the open squares and the open circle at $I = 14$ $\hbar$ have been deduced by using the $B(E2)$ values reported in [11]. According to eq. (4), in case the measured relative $B(E2)$ values are equal to the respective ones predicted by the vibrational limit (U(5)-limit) of IBM-1, then the respective data points $R(I)$ have to lie on the straight line labeled in fig. 8 with letter a. This line correspond to $R(I) = 1$. Curve labeled "b" represent the ratio of the relative $B(E2)$ values predicted by the SU(3) limit of IBM-1 (rotational limit) to those predicted by the U(5) limit.

121

In fig. 8, more than one data point are shown for spins $I = 8, 10, 12$ $\hbar$, in accordance to level scheme of ^{110}Cd (see fig. 7). Hereby, the number in parenthesis is the energy in keV of the γ-transition in consideration. As it can be seen in fig. 8 the data points for $I = 2, 4, 6$ $\hbar$ lie statistically on the straight line "a". For $I = 8$ $\hbar$, one has to distinguish between the weak $8_1^+ \rightarrow 6_1^+$ γ-transition (E_γ=707 keV) and the strong $8_2^+ \rightarrow 6_1^+$ γ-ray (E_γ=795 keV). The data point of the latter transition lies indeed on line "a", whereas the data point of the former γ-ray deviates strongly from R=1. For $I = 10$ $\hbar$ the relative $B(E2)$ values of two γ-transitions are close to the respective U(5) predictions. These two γ-transitions are the $10_2^+ \rightarrow 8_2^+$ (E_γ=802 keV) and the $10_1^+ \rightarrow 8_3^+$ (E_γ=171 keV). In contrast to these γ-rays, the data points of the $10_1^+ \rightarrow 8_2^+$ (E_γ=335 keV), $10_2^+ \rightarrow 8_3^+$ (E_γ=637 keV), and $10_1^+ \rightarrow 8_1^+$ (E_γ=424 keV) γ-transitions deviate strongly from the straight line "a". For $I = 12$ $\hbar$ the relative $B(E2)$ value of the $12_1^+ \rightarrow 10_1^+$ (E_γ=561 keV) γ-ray coincides with the value predicted by the U(5) limit [$R_{12_1^+} = 1.00(5)$], whereas the data point for $12_2^+ \rightarrow 10_2^+$ (E_γ=811 keV) γ-transition is very close to line "a" [$R_{12_2^+} = 0.90(5)$]. At $I = 14$ $\hbar$, the relative $B(E2)$ value reported in [11] for the $14_1^+ \rightarrow 12_1^+$ (E_γ=854 keV) γ-ray is slightly higher than this expected by the U(5) limit.

Based on fig. 8, and provided that the $8_2^+ \rightarrow 6_1^+$ (E_γ=795 keV) γ-line, together with the "unfavoured" pathway consisted of the 802 keV and 811 keV γ-rays are the continuation of the ground band, one clearly sees that the level sequence
$$2_1^+, 4_1^+, 6_1^+, 8_2^+, 10_2^+, 12_2^+$$
forms a nice vibrational band with intraband $B(E2)$ values being in agreement with the predictions of the U(5) limit of IBM-1.

In addition to the above mentioned points and according to the experimental $B(E2)$ values measured for the $10_1^+ \rightarrow 8_2^+$, $12_1^+ \rightarrow 10_1^+$, and $14_1^+ \rightarrow 12_1^+$ γ-transitions, the sequence
$$10_1^+, 12_1^+, 14_1^+$$
seems to be a rotational-like S-band. Hereby, the character of the long lived 10_1^+ state is of great importance. This state most probably represent a fully aligned $h_{11/2}$ neutron pair, as claimed in [11]. This could be definately confirmed via a g-factor measurement of this state.

5 Summary

In the present work the mean lifetimes of the lowest six yrast band members of ^{110}Cd have been measured. Using these data it was possible to follow the evolution of the $B(E2)$ values along the yrast line of the nucleus up to the 12_1^+ state.

In general, the final "picture" obtained for the ^{110}Cd nucleus is in agreement with the predictions of the U(5) limit of IBM-1: ^{110}Cd seems to be indeed one of the best cases of vibrational nuclei.

Additional lifetime and/or g-factor measurements could provide valuable assignments on the character of the excited levels and further elucidate the interplay between rotational and vibrational excitations in the nucleus considered.

<div align="center">

Table 1

</div>

Spin J_i^π	Level E_x (keV)	Side feeding intens. (%)	mean lifetime τ (ps) this work	others[a]	γ-ray E_γ (keV)	Intensity (arb. units)	Branching (%)	B(E2) [W.u] this work	others[a]
2^+	658	0.5(24)	8.7(12)	7.78(10)[b]	658	100	100	24^{+3}_{-3}	27(1)[b]
				9.2(6)					23.0(15)
4^+	1542	3.5(21)	1.0(5)	1.05(13)[b]	885	99.5(2)	100	48^{+48}_{-16}	46(6)[b]
6^+	2480	2.4(22)	0.9(5)		938	82.1(1)	100	40^{+50}_{-14}	
8^+	3275	0.1(25)	1.5(5)		795	50.5(8)	100	55^{+27}_{-14}	
10^+	3611	20.2(36)	670(25)	800(40)	335	40.5(9)	71.9(26)	$6.6^{+0.4}_{-0.3}$	6.0(3)
					171	11.5(13)	20.4(24)	45^{+5}_{-5}	26(2)
					424	0.9(3)	1.7(7)	$0.05^{+0.02}_{-0.02}$	0.04(1)
					265	3.4(5)	6.0(1)		
12^+	4172	23.1(38)	11.4(6)	12.0(6)	561	44.9(11)	100	41^{+2}_{-2}	39(2)
14^+	5026		< 3	2.0(2)	854	34.5(12)	100	> 16	29(3)
10^+	4078		< 4	1.0(3)	802	13.9(4)	100	> 19	74(24)
5^-	2540		< 885(120)		998	13.9(4)			
7^-	2879		< 1018(101)	1000(60)	399	22.1(5)			

[a] Reported in ref. [11], if not explicity given.

[b] Reported in ref. [12]

References

[1] A. Arima and F. Iachello, Ann. Phys. **99**(1976)253.

[2] T.K. Alexander and J.S. Foster, Adv. Nucl. Phys. **10**(1978)197.

[3] P.J. Nolan and J.F. Sharpey-Schafer, Rep. Prog. Phys. **42**(1979)1.

[4] H. Hanewinkel, Diplomarbeit, Unstitut für Kernphysik, Universität zu Köln, Köln 1981, unpublished.

[5] A. Dewald, S. Harissopulos and P. von Brentano, Z. Phys. **A334**(1989)163.

[6] G. Böhm, A. Dewald, P. Petkov and P. von Brentano, Nucl. Instr. Meth. **A329**(1993)248.

[7] A. Dewald, U. Kaup, W. Gast, A. Gelberg, H.W. Schuh, K.O. Zell and P. von Brentano, Phys. Rev. **C25**(1982)26.

[8] C.M. Lederer and V.S. Shirley, eds., Table of isotopes, J. Wiley & Sons, (New York, 1978).

[9] F. Seiffert, program APATHIE, Institut für Kernphysik, Universität zu Köln, Köln 1989, unpublished.

[10] S. Harissopulos, A. Dewald, A. Gelberg, P. von Brentano, K. Loewenich, K. Schiffer and K.O. Zell, Nucl. Phys **A467**(1987)528.

[11] M. Piiparinen, R. Julin, S. Juutinen, A. Virtanen, P. Ahonen, C. Fahlander, J. Hattula, A. Lampinen, T. Lönnroth, A. Maj, S. Mitarai, D. Müller, J. Nyberg, A. Pakkanen, M. Sugawara, I. Thorslund and S. Törmänen, Nucl. Phys. **A565**(1993)671.

[12] D. De Frenne and E. Jacobs, Nucl. Data Sheets **67**(1992)809.